IEEE Access
Multidisciplinary | Rapid Review | Open Access Journal

Received March 18, 2019, accepted April 1, 2019, date of publication April 11, 2019, date of current version April 23, 2019.

Digital Object Identifier 10.1109/ACCESS.2019.2910376

Switch-Reconfigurable Metal Rim MIMO Handset Antenna With Distributed Feeding

RASMUS LUOMANIEMI, (Student Member, IEEE), JARI-MATTI HANNULA, (Member, IEEE), ANU LEHTOVUORI, AND VILLE VIIKARI, (Senior Member, IEEE)

Department of Electronics and Nanoengineering, Aalto University School of Electrical Engineering, FI-00076 Espoo, Finland

Corresponding author: Rasmus Luomaniemi (rasmus.luomaniemi@aalto.fi)

This work was supported by the 5G TRx Project funded in part by Business Finland, in part by Nokia Bell Labs, in part by Huawei Technologies Finland, in part by RF360, in part by Pulse Electronics Finland, and in part by Sasken Finland.

ABSTRACT A new antenna design method together with a novel metal rim antenna is presented in this paper. The design method transforms an electromagnetic synthesis problem into a circuit problem, which can be solved in a straightforward manner. The new metal rim antenna is based on switches and the antenna cluster concept. The antenna cluster concept uses several, differently fed radiating elements together as one antenna. The proposed method is used to design a handset antenna with small ground clearance of 5 mm capable of 2×2 MIMO operation in the 698–960 MHz low band with 30–40 % efficiency and 4×4 MIMO in the 1.7–2.7 GHz middle-high band with better than 50 % efficiency, and the 3–4 GHz high band with efficiency up to 75 %. The proposed optimization method leads to a novel way of distributing the antennas over the entire available volume.

INDEX TERMS Frequency-reconfigurable, metal rim, mobile antennas, multiple-input multiple-output (MIMO), RF-switches.

I. INTRODUCTION

Designing efficient MIMO antennas for all the frequency bands needed in 5G requires an enormous number of time-consuming electromagnetic (EM) simulations, but repeating similar simulations does not create new and innovative solutions. New methods are needed to find different perspectives and also to accelerate the design process. At the same time, the practical aspects of handsets have to be taken into account in the design process.

Traditionally, designing antennas requires a large number of EM simulations to optimize both the location and the geometry of the antenna elements [1]–[5]. Especially self-resonant antennas tend to have complicated structures that require a lot of optimization, often performed manually by the antenna designer [6]–[12]. By using non-resonant antennas, such as capacitive coupling element antennas (CCEs) [13], the geometry of the antenna element is simpler and part of the problem is transformed into finding a proper matching network [14]. The operation of different frequency bands are usually designed separately [15] and the EM simulation is iterated several times for each frequency band. Especially if a more detailed simulation model is used, the EM simulations take a long time.

Antenna design methods based on numerically optimizing the size and shape of the metallic radiating structure have been proposed, e.g., in [16], [17]. These methods can produce antennas with arbitrary shapes which are not necessarily applicable in consumer devices because of practical aspects.

This paper, based on [18], proposes a new optimization method that requires only one EM simulation. By using a multiport antenna simulation model and an evaluation algorithm, the EM synthesis problem is transformed into a circuit problem allowing to evaluate a large number of different antenna structures in a short time. Different antenna structures are created from the multiport antenna model by placing the feeds, open circuits, and short circuits into the available ports and finding the combination that gives the best performance. Because of the design method, the designer does not have to make any major assumptions about the sizes or locations of the antenna elements beforehand. This kind of optimization with current commercial EM simulators would require a very large number of time-consuming simulations making it impractical option in many cases.

The associate editor coordinating the review of this manuscript and approving it for publication was Guan-Long Huang.

Using the whole metal frame as an antenna has been a popular option because of its appealing appearance and mechanical strength. Adding a metal rim into the device has a large effect on the traditionally used internal antennas [19]. Many different types of designs for metal rimmed devices have been published in the recent years [20]–[28]. However, many of these designs require impractically large ground clearances for modern smartphones. In addition, most of the designs do not support MIMO operation or the 3.5 GHz band for 5G.

To efficiently utilize the metal rim and to allow distributed feeding, we apply antenna cluster technique [29]–[32] where a set of antenna elements is used as one antenna by feeding ports with complex weighted signals. By optimizing the structure separately for different frequency bands, the optimal size and number of antennas can be used on each band. For practical realization, the structures for different frequency bands are created with switches. The proposed method allows the utilization of the available volume more efficiently and also achieving a high data rate by using higher order MIMO in middle-high and high bands compared with the traditionally used two-element MIMO [4], [5], [33].

In addition to this novel design method, which accelerates the design process and helps designers to find novel solutions without being limited by traditional assumptions, this paper presents a new antenna type making it possible to realize high-order MIMO antennas whose frequency can be reconfigured across a large band. The effectiveness of the proposed method is demonstrated by designing a high-capacity MIMO antenna system for a mobile device with metal rim. The antenna proposed in this paper is one of the few published designs that can cover the low band with two-element MIMO and higher bands with four-element MIMO in a form suitable for modern smartphones with very small ground clearances. The measurement results confirm that a good performance is achieved.

II. BACKGROUND

The goal of the proposed method is to utilize the metal rim of a handset as antenna clusters. The structure is reconfigured for different frequency bands with switches. The locations of the feeds, short circuits, and open circuits are found using an evaluation algorithm and a multiport simulation model built from small unit antenna elements, like the one shown in Fig. 1. The algorithm evaluates different combinations and selects the best one. The MIMO capacity is used as a figure-of-merit to find the best structure.

A. THE ANTENNA CLUSTER CONCEPT

The antenna cluster concept initially presented in [29], [30] uses several antenna elements that are fed with complex weighted signals to maximize the combined efficiency of the cluster. The antenna cluster can be tuned to operate at different frequencies by adjusting the feeding weights accordingly for each frequency point.

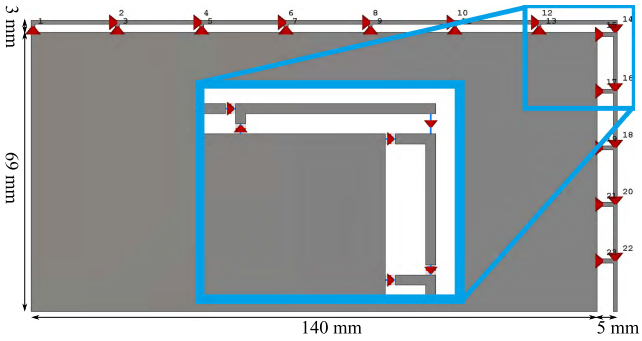

FIGURE 1. L-shape multiport antenna simulation model with a close-up of the unit antenna elements. Red ports indicate possible positions for feeds, open circuits, or short circuits.

With incident wave vector $\mathbf{a}$, the matching efficiency η_{match} of an antenna cluster with scattering parameters $\mathbf{S}$ is

$$\eta_{\text{match}} = \frac{\mathbf{a}^{\text{H}}(\mathbf{I} - \mathbf{S}^{\text{H}}\mathbf{S})\mathbf{a}}{\mathbf{a}^{\text{H}}\mathbf{a}}, \tag{1}$$

where $()^{\text{H}}$ is the conjugate transpose. The performance of the antenna cluster is determined by the matrix $\mathbf{I} - \mathbf{S}^{\text{H}}\mathbf{S}$. The maximum obtainable active matching efficiency can be calculated by finding the largest eigenvalue, i.e.,

$$\eta_{\text{match,max}} = \max\left\{\text{eig}(\mathbf{I} - \mathbf{S}^{\text{H}}\mathbf{S})\right\}, \tag{2}$$

which is obtained when $\mathbf{a}$ is the eigenvector corresponding to the maximum eigenvalue [29]. Eq. (2) is later used to pre-evaluate different structures using the S-parameter model of the antenna.

Using the S-parameters to calculate the feeding weights does not take losses of the structure into account and maximum obtainable performance might not be achieved. Also, measuring the S-parameters of a multiport antenna is laborious. These problems can be solved by replacing $\mathbf{I} - \mathbf{S}^{\text{H}}\mathbf{S}$ in Eq. (2) with matrix $\mathbf{D}$ calculated from the far-field patterns of each antenna element. The elements of $\mathbf{D}$ are

$$D_{ij} = \iint_{4\pi} F_i \cdot F_j^* \, d\Omega \tag{3}$$

and F_i is the radiation pattern of ith feed port [34]. Eq. (3) is later used to evaluate the total efficiency and MIMO capacity.

B. MIMO

In this work, the MIMO capacity is used to compare different antenna designs by taking into account the operation of the whole antenna system instead of just the efficiencies of individual antennas. It should be noted that when using antenna clusters, one antenna cluster corresponds to one antenna for the MIMO system as in [32]. The total radiation pattern for each stream is then

$$F_{\text{tot}} = \sum_{n=1}^{N_f} \alpha_n F_n, \tag{4}$$

where N_f is the number of feeds in an antenna cluster and α_n is the complex weighting coefficient for each element in a cluster calculated using (2) and (3).

The different antenna designs can be compared by calculating the MIMO capacity C for each case. In this paper, the capacity is calculated following [35] as

$$C = \log_2 \left(\det \left(\mathbf{I}_M + \frac{\mathrm{SNR}}{M} \mathbf{H}\mathbf{H}^{\mathrm{H}} \right) \right), \tag{5}$$

where M is the number of transmitter and receiver antennas, $\mathbf{H}$ is the channel matrix, and SNR is the signal-to-noise ratio. Rayleigh fading channel $\mathbf{H}_w$ describing a rich scattering environment modelled with independently and identically distributed complex Gaussian random variables is assumed. The MIMO channel matrix $\mathbf{H}$ is then calculated as

$$\mathbf{H} = \mathbf{R_r}^{1/2} \mathbf{H}_w, \tag{6}$$

where $\mathbf{R_r}$ describes the effect of the receiving antennas, including efficiency, coupling, and correlation, calculated from the radiation patterns of the clusters [35]. It should be noted that (6) only takes into account the effect of the receiving handset antennas and assumes ideal transmitting antennas.

Instantaneous capacity calculated from (5) is valid for only one channel realization. Ergodic capacity is the average capacity calculated with a large number of independent channel realizations [36]. In this paper, ergodic capacities are calculated with 5000 channel realizations and with SNR = 20 dB which are commonly used parameter values [37], [38].

III. PROPOSED OPTIMIZATION METHOD

A. MAIN IDEA OF THE DESIGN METHOD

The design method uses a multiport antenna simulation model built from a large number of small unit antenna elements. Each of these elements has one feed port and the different unit elements can be connected or disconnected with short circuits or open circuits. The evaluation algorithm finds the optimal combination of feeds, open circuits, and short circuits. Fig. 2 illustrates an example of placing two feeds and three open circuits into a simulation model with four unit antenna elements.

Using reactive loading to ground the antenna element is known to improve the performance especially at the low frequencies [26], [39]. The proposed method also allows the ports to be terminated with inductors and capacitors. However, this would increase the complexity significantly because the component values for each element should also be optimized, and therefore, is out of scope of this paper.

With antenna clusters, both matching of individual ports and coupling between the ports have a significant effect on the performance. The operation of the entire antenna cluster can be characterized with a single figure with matching efficiency and it can be calculated directly from the S-parameter model using (1). Therefore matching efficiency is used to pre-evaluate different antenna structures to find the most promising ones. The final optimization goal is the MIMO capacity. This computationally more demanding capacity is then calculated only for the best candidates based on the matching efficiency.

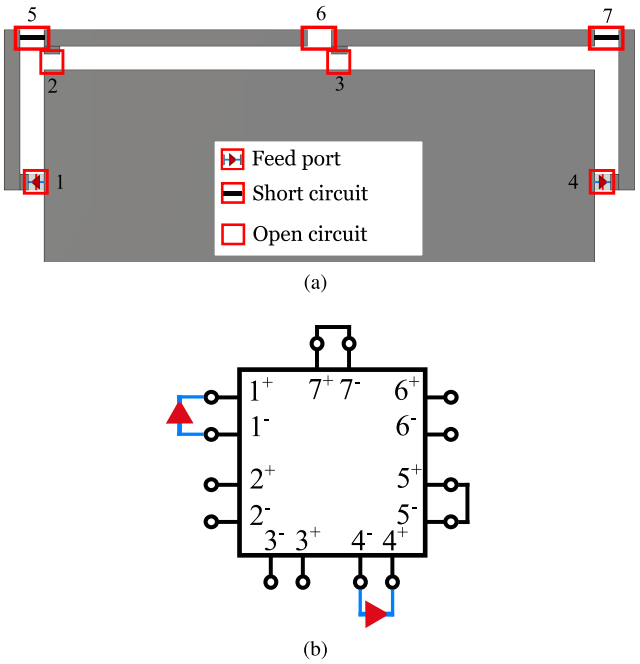

FIGURE 2. Simplified presentation of the basic principle of the evaluation algorithm. (a) Electromagnetic simulation model with ports shown as red squares and (b) corresponding circuit simulation model.

The antenna structure is optimized separately for different frequency bands. If a port is terminated differently in different bands, a switch is used to modify the structure for each case.

B. NOVELTY AND BENEFITS OF THE DESIGN METHOD

By applying the evaluation algorithm for the EM simulation model consisting of unit antenna elements, a large number of different antenna structures can be studied with only one EM simulation by transforming the problem into a circuit problem. Because circuit simulation is considerably faster than EM simulation, the design process can be accelerated significantly.

Most commercial EM simulators have optimization features that can be used to find optimal structures. However, these tools work usually fine for fine-tuning when the approximate structure is already known but for finding completely new solutions, they are inefficient in most cases. Using the proposed multiport simulation method, the designer does not have to make any assumptions about the size, location, or even the number of antenna elements forming the antenna clusters. This makes it possible to find radically new designs that would otherwise be difficult to find using the traditional design methods.

By optimizing the structure for each frequency band separately with switches, the limited volume available for antennas is used as efficiently as possible. Lower frequencies are more challenging to implement in a limited volume. For this reason, the low band structure optimization is performed first. The higher frequency structure is optimized after the low band structure has been designed and in this optimization, the low band structure is kept fixed. This makes it possible

to use the low-band open circuits also for higher frequencies. Thus, the number of switches is minimized and a good low-band performance is retained.

C. DETAILS OF THE METHOD WITH THE PROPOSED DESIGN

In this paper, the proposed method is demonstrated by designing a MIMO antenna system for a mobile device. To limit the computation time, the optimization for matching efficiency is performed for a simulation model where unit elements are placed such that they cover only half of the perimeter of the ground plane as shown in Fig. 1. The full metal rim structure used for the total efficiency and capacity evaluations is then obtained by copying these antenna elements. After the structure has been optimized for all frequency bands, the final phase is to fine tune the whole structure. The final optimization is performed because the structure is modified when the unit elements are combined into actual antenna elements and the unused feed lines are removed. Also, the size of the unit elements determine the accuracy at which the feed and switch placement can be found. The final optimization is performed to take these factors into account. The general design process utilized in this case is presented in Fig. 3.

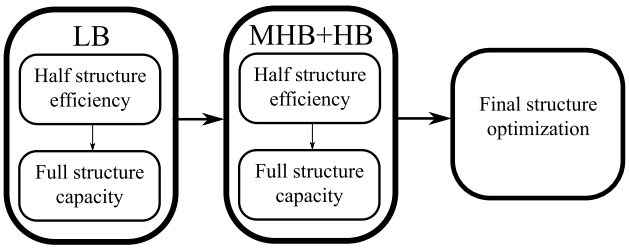

FIGURE 3. General design process of the proposed method.

The goal of the evaluation algorithm is to find the optimal placement of the feeds and switches. The algorithm uses the S-parameter model of the multiport antenna simulation model. The design parameters are:

- frequency band
- the number of data streams N_T
- number of feeds in an antenna cluster N_f
- number of open circuits N_{oc}.

First, all possible combinations of placing $N_T \times N_f$ feeds to the available feed ports are created. Next, all possible combinations of placing N_{oc} open circuits in the metal rim are created. In this work, additional constraints can be used for the middle-high and high bands to force the algorithm to use the same feeds and switches that are used in the low band.

Next, all possible feed, open circuit, and short circuit combinations are evaluated. The S-parameter model of the antenna is modified such that unused feed ports are set to open circuits, i.e., terminated with infinite impedance. If the used MIMO configuration is 2×2, one antenna cluster is built into the half structure. If more data streams are used, S-parameter models with corresponding feed ports are created for each stream while the feeds of other streams are terminated with 50 Ω. The matching efficiency for each data stream is calculated using (2) and the best options are chosen.

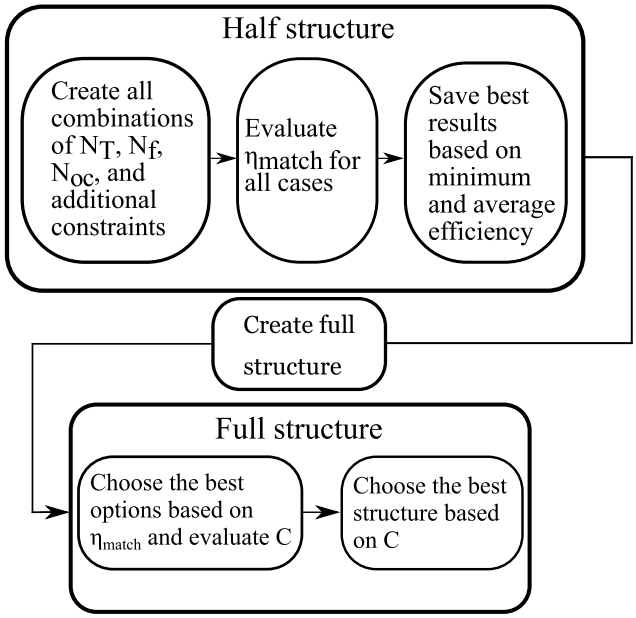

FIGURE 4. Flowchart of the evaluation algorithm.

The final phase is to calculate the capacity for the best options based on the matching efficiency. The far-field patterns of each element in one cluster are first summed with the complex weights using Eq. (4) and these patterns are used to calculate the capacity according to Eq. (3) and Eq. (5). Fig. 4 presents the evaluation algorithm performed at each frequency range in Fig. 3.

It should be noted that although in the design presented in this paper we are using a simplified model of a mobile device and a symmetric antenna configuration, the design method in general is not limited by these factors. The multiport simulation model could include, e.g., internal components of the phone and the optimization could also be performed directly for the full model instead of the half structure.

IV. DESIGN PROCESS OF A MOBILE ANTENNA

The proposed design method is first applied to a simulation model consisting of an infinitely thin PEC ground plane and the antenna unit elements. The size of the ground plane is 140×69 mm^2. Current trends in commercial smartphones require as small as possible clearances and therefore 5 mm and 3 mm are chosen. The ground clearance is measured from the edge of the ground plane to the outer edge of the metal rim on the same plane as shown in Fig. 1. The total dimensions of the full antenna models are then 150×75 mm^2, which correspond to, e.g., Apple iPhone 8 Plus and Huawei Mate 10 Pro.

To implement two-element MIMO in the low band, five ways to split the volume into two half structures are considered. Based on the appearance of the antenna elements, these models are called L-shape, U-shape and three versions of J-shape. The L-shape model is shown in Fig. 1 and the

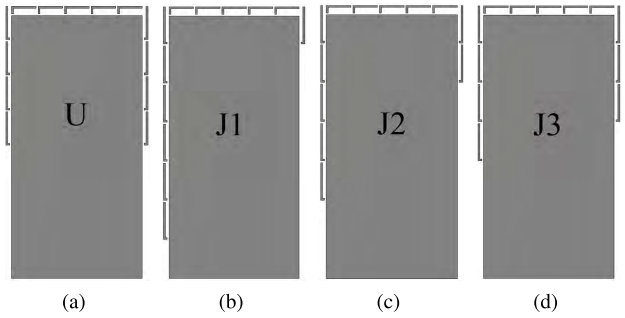

FIGURE 5. Other antenna shapes used in the initial study: (a) U-shape, (b) J1-shape, (c) J2-shape, and (d) J3-shape.

other models in Fig. 5. The length of the unit element on the long edge is 19.86 mm for the L-shape and the J-shape models and 17.75 mm for the U-shape model. The length of the unit element on the short edge is 13 mm for all models. The width of the element is 1 mm and the gap between the elements is 1 mm. There are 12 unit elements in the L- and J-shape models and 13 in the U-shape model.

A. LOW-BAND OPTIMIZATION

For the low-band half-structure optimization, $N_T = 1$, N_f gets values from one to two and N_{oc} from zero to three. From the resulting half structures, three of the most promising ones for each shape are chosen for the full structure capacity calculation. The best capacities and total efficiencies for each case are shown in Fig. 6. The ideal capacity is the upper limit of achievable capacity that is achieved when all antennas are 100 % efficient and there is zero correlation between them [35].

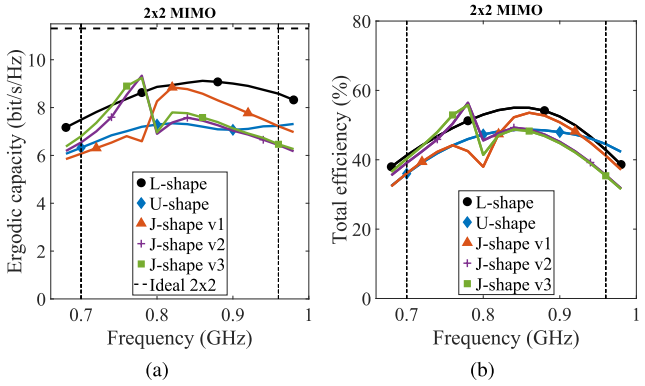

FIGURE 6. (a) MIMO capacities and (b) total efficiencies for different antenna models in the low band.

Based on the obtained results, the L-shape gives the best performance. The capacity across the whole band is rather flat and the level is the highest. Therefore, the L-shape model is chosen for the middle-high and high-band optimization.

B. MIDDLE-HIGH AND HIGH-BAND OPTIMIZATION

The middle-high and high-bands are studied together. The low-band feeds are used to keep the structure as simple as possible. The open and short circuits for the middle-high and high-band structure can be designed completely independently of the low-band structure or they can be co-designed by forcing the algorithm to use the same open circuits that are used in the low-band. Both options are considered.

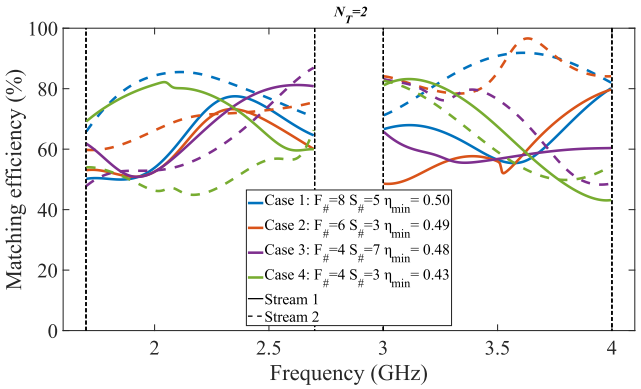

FIGURE 7. Matching efficiencies for different two data stream structures. Efficiencies of different data streams with different line types.

The low band can practically use only two MIMO antennas but at higher frequencies, more data streams can be utilized. Therefore, the effect of increasing N_T is studied. Fig. 7 shows the matching efficiency results for the $N_T = 2$ case. $F_\#$ is the total number of feeds, $S_\#$ is the total number of switches required, and $\eta_{\min}$ tells the minimum efficiency for each case. The results show that using more than two feeds per data stream (i.e., $F_\# = 4$) does not produce significant improvement. Similar results are found for the cases $N_T = 3$ and $N_T = 4$ also.

The results for higher number of data streams show that it is possible to have several separate data streams in the half structure. However, Table 1 shows that as N_T is increased, the minimum efficiency decreases.

TABLE 1. Comparison of number of data streams and minimum efficiencies for MHB and HB.

N_T	$F_\#$	$S_\#$	$\eta_{\min}$
2	4	3	0.43
3	6	3	0.38
4	8	5	0.31

The benefit of co-designing the low-band and high-band structures can be seen from cases 3 and 4 in Fig. 7. In both cases, $N_{oc} = 5$ but the total number of switches needed are seven and three. When the same ports are set to open circuits in all frequency bands, they can be replaced with gaps in the antenna structure without actual switches. Since the performance of the two cases are quite similar, it is beneficial to minimize the total number of switches used.

Next, the capacity is evaluated for the different MIMO configurations. For each case, $N_f = 2$ and minimum $S_\#$ that gives reasonable efficiency performance are chosen. The results and the corresponding ideal capacities are shown in Fig. 8. Although the minimum efficiency decreases with increasing N_T, the capacity increases. However, when comparing each case with the corresponding ideal capacity, the achieved capacity decreases.

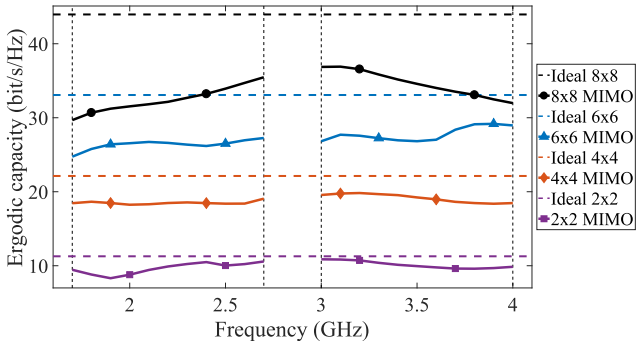

FIGURE 8. Obtained capacity performance for different MIMO configurations compared to ideal capacities.

C. PROPOSED DESIGN

The MIMO configurations chosen based on the initial study are 2×2 for the low band and 4×4 for middle-high and high bands. The 4×4 is chosen because it provides relatively good performance without too large number of switches. It can be expected that the larger number of switches required by, e.g., the 8×8 case will be affected more than the 4×4 case when realistic switches are taken into account.

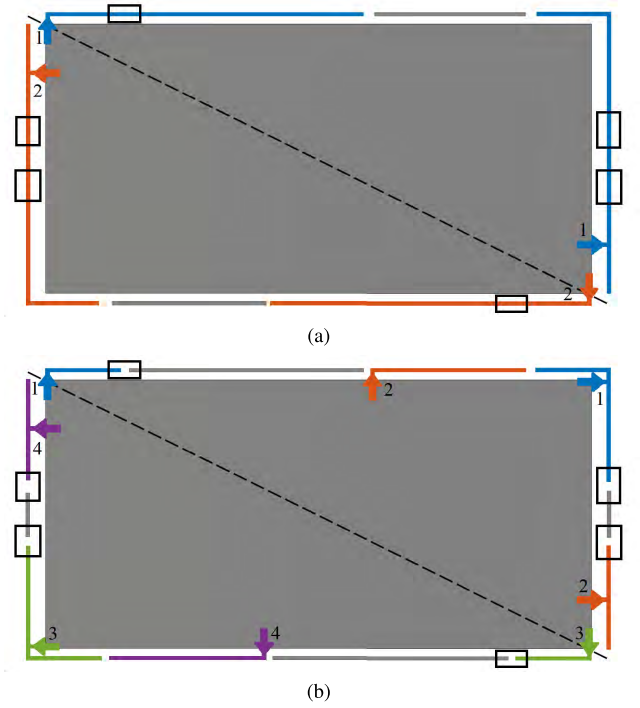

FIGURE 9. The antenna structures for the (a) low band and (b) middle-high and high bands. The dashed line denotes the symmetry plane. Locations of closed switches in (a) and open switches in (b) are shown with black rectangles. Different antenna clusters and their feeds are shown with different colors and numbering.

The antenna structures are presented in Fig. 9. The proposed approach leads to a new way of placing the antennas: elements are distributed along the entire metal rim of the device. The low band uses two large antenna elements on the long and short edges of the ground plane and one parasitic element between them. The middle-high and high-band structure has four smaller antenna elements and two parasitic elements. With switches, larger elements can be used for the low band while a larger number of smaller elements can be utilized at higher frequencies.

As a demonstration of the benefits of the proposed method, the presented low-band optimization evaluates over 18000 different structures. With traditional approach, the simulation time is exponentially related to the number of ports whereas with the proposed method, the simulation time increases only linearly with the total number of ports. In this case, the proposed method is at least one order of magnitude faster. Using larger number of feed ports, like in the middle-high and high-band optimization, or simulating a more complex structure than just a PEC sheet further increases the difference and makes the proposed method more attractive.

V. PROTOTYPE AND MANUFACTURING

To use the maximum volume available for the antennas, and to build the antennas into the metal rim of the phone, the simulation model has a 4 mm high metal rim. Also, for practical realization, a 0.8 mm-substrate is added. The substrate material is chosen to be Rogers RO4003C with dielectric constant $\varepsilon_r = 3.38$ and dissipation factor $\tan\delta = 0.0021$ (2.5 GHz/23°C). All the gaps between the antenna elements are 1 mm wide.

The placement of the feeds and switches for the final structure are found based on the results of the initial study. After this, the unused feed lines are removed and larger uniform antenna elements are formed. The final optimization of the placement of the feeds and the gaps in the antenna structure is performed to get the best possible performance in all frequency bands.

For the complete model of the antenna, the ideal switches need to be replaced with real ones. The most common types of RF switches are PIN diode switches, field-effect transistor (FET) switches and microelectromechanical systems (MEMS) switches [40], [41]. The most important switch characteristics considered in this paper are the insertion loss and the isolation. Other factors, such as switching speed, are not considered here. Different switch models are studied with simulations and the best option based on the performance and the manufacturability is Skyworks SMP1345-040LF PIN diode. Both simulations and measurements use 0 V reverse bias voltage and 10 mA forward bias current. The voltages and the power dissipation of the diodes are studied by circuit simulations to make sure that they do not break down. With power levels used for mobile devices, the diode voltages and power levels are well below the manufacturer specified maximum ratings.

The full switching circuits are implemented on the PCB. Unused high-band feeds are switched off in the low band to make them look open circuits for the low-band feeds. In addition to the PIN diode, the switches also need bias networks to isolate the RF signal and the bias voltage. The bias networks are realized with Murata GQM1882C1H510GB01

51 pF DC block capacitors and LQW18ANR20G00 200 nH RF choke inductors. The DC block capacitors and RF choke inductors have been chosen to provide relatively low and high impedances, respectively, at the operating frequencies [42]. Because of the total size required by the switching circuits, they are realized partly on the ground plane instead of directly between the antenna elements. Fig. 10 shows the bias networks designed for the diodes.

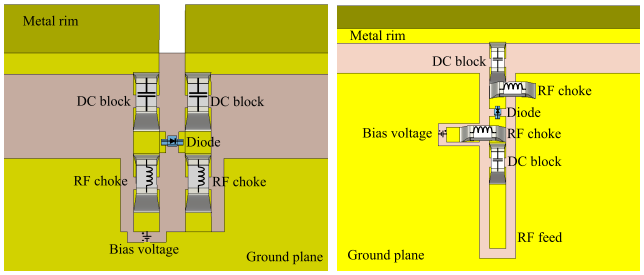

FIGURE 10. Implemented switching circuits for (a) metal-rim switches and (b) switched feeds.

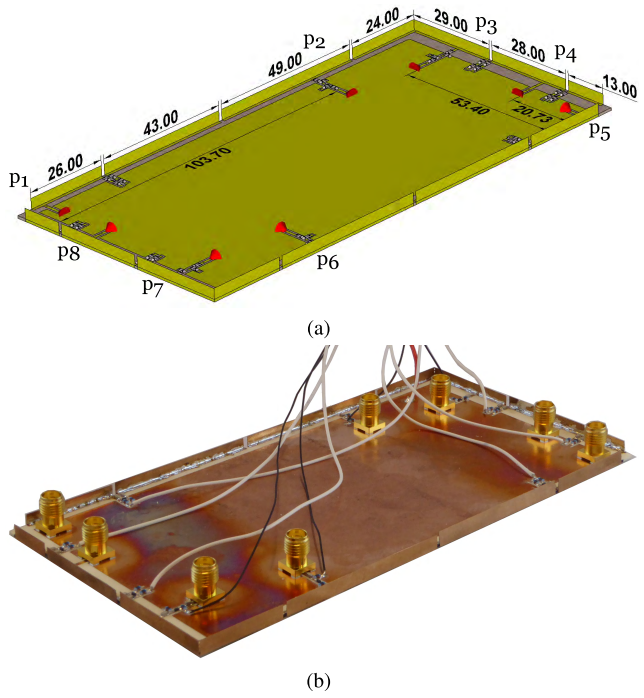

FIGURE 11. Proposed antenna design, (a) simulation model and (b) manufactured prototype. All dimension are in millimeters.

Fig. 11(a) shows the resulting final simulation model and Fig. 11(b) the manufactured prototype of the antenna. The configurations for the antenna clusters are presented in Table 2 with port numbering referring to that of Fig. 11(a).

VI. RESULTS AND DISCUSSION

A. RESULTS

The measurements are performed with MVG StarLab 6 GHz antenna measurement system. The far-field patterns are measured one feed at a time while the other feeds are terminated with 50 Ω loads. The individual radiation patterns are then used to calculate the optimal feeding weights and the total efficiency and the MIMO capacity are calculated from the combined field patterns as explained in Section II.

TABLE 2. Antenna cluster configurations.

LB	Data stream	1		2	
	ports	p_1, p_4		p_5, p_8	
HB	Data stream	1	2	3	4
	ports	p_1, p_2	p_3, p_4	p_5, p_6	p_7, p_8

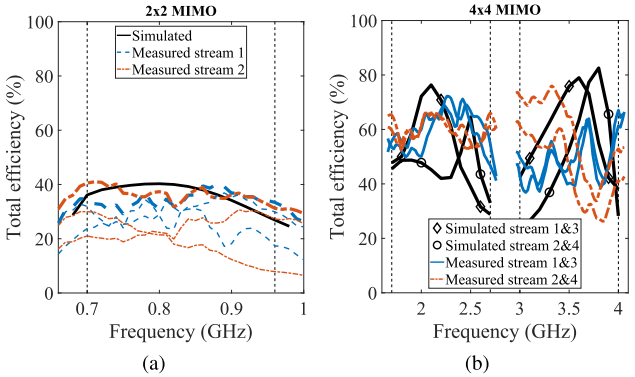

FIGURE 12. Measured and simulated total efficiencies in (a) low band and (b) middle-high and high bands. In (a), weighted antenna cluster results are shown with thick lines and measured individual antenna elements with thin lines.

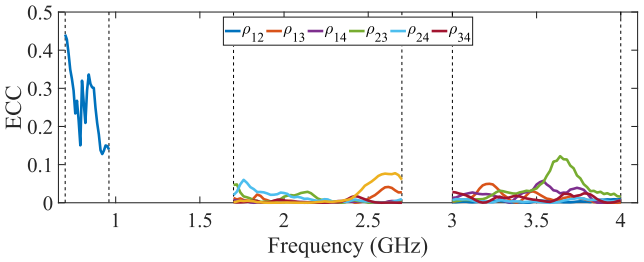

FIGURE 13. Measured envelope correlation coefficients.

The total efficiency and envelope correlation coefficient (ECC) results are shown in Fig. 12 and Fig. 13 and the capacity results calculated from the antenna properties in Fig. 14. The measurement results for the low band and the middle-high band are in good agreement with the simulation results. In the high band, there is a larger difference between the measurements and simulations. This is likely caused by manufacturing inaccuracies that are affecting the high band most because of the shorter wavelength. The maximum ECC is 0.44 in the low band. The results show that correlation is below 0.5 in all frequency bands, which is usually considered as low correlation [35].

The achieved total efficiency and MIMO capacity for the 2 × 2 low band are 30–40 % and about 8 bit/s/Hz. For the 4 × 4 middle-high band, 50–70 % efficiency

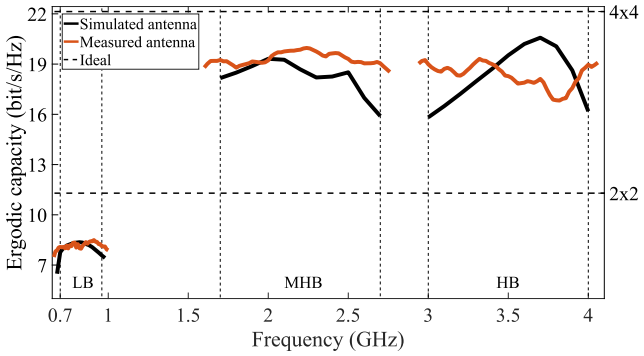

FIGURE 14. MIMO capacities calculated using simulated and measured antenna properties.

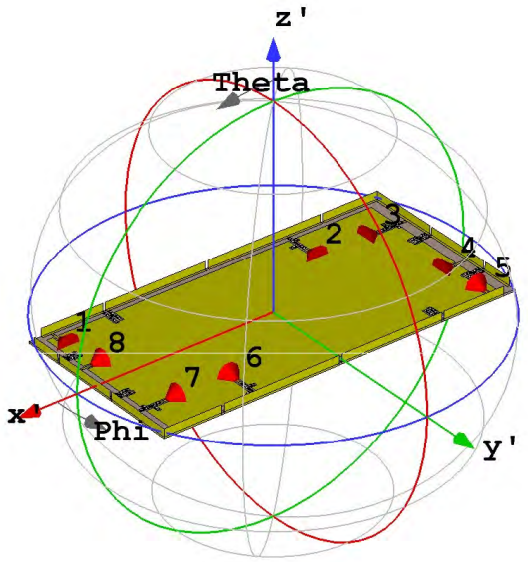

FIGURE 15. Orientation of the device and the used coordinate system.

and 19–20 bit/s/Hz capacity are achieved and 25–75 % efficiency and 17–19 bit/s/Hz capacity for the high band. As far as authors know, this is the first published design with 4 × 4 MIMO in the middle-high and high bands that also covers the low band with 2 × 2 MIMO in a size suitable for modern smartphones. All high-band antennas achieve competent efficiency.

In addition to the ECC, the spatial diversity performance of the proposed design can be studied from the radiation patterns of the antennas. The orientation of the device and the coordinate system in which the results are presented is shown in Fig. 15 and the low-band and middle-high-band radiation patterns for all data streams are shown in Fig. 16 and Fig. 17. The results show that by distributing the antenna elements around the whole metal rim, broad spatial coverage is achieved.

The feeding weights for the low band elements are shown in Fig. 18. In the phase results, feed 1 is chosen as a reference, i.e., it is always 0°. The low band feed coefficients and the individual element efficiencies in Fig. 12(a) clarify the operation principle of the low band antenna clusters. The cluster is formed by two antennas with different resonant frequencies, around 700 MHz and 900 MHz. By adjusting the

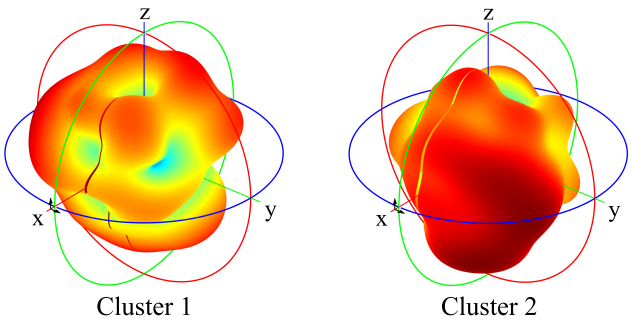

FIGURE 16. Measured low-band radiation patterns at 830 MHz.

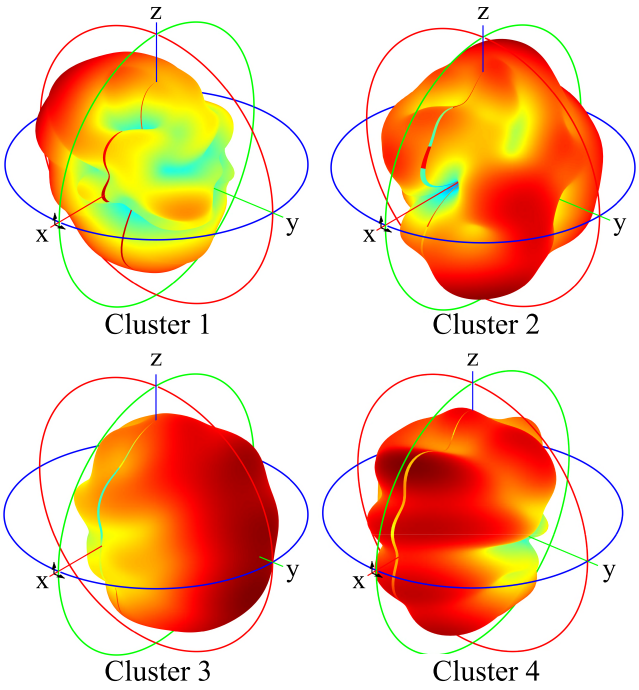

FIGURE 17. Measured middle-high-band radiation patterns at 2200 MHz.

amplitude and phase of the input signal between these two antennas properly, the whole low band can be covered with better efficiency than either of the individual elements used alone.

The feeding weights of data streams 1 and 2 for the middle-high and high bands are shown in Fig. 19. Results for streams 3 and 4 are similar. Both frequency bands can be covered by properly adjusting the signals of the two feeds of an antenna cluster. Because the low-band feeds were chosen to be used also in the middle-high and high bands, the optimal usage of the antenna clusters is not necessarily possible. However, the results show that all antenna elements are used although, e.g., stream 2 high band is mostly covered with feed 2.

Table 3 presents a comparison of the proposed antenna with some recently published antenna designs. The two clearance values correspond to those along the short edge and the long edge of the device, respectively. The proposed design has several benefits over the others. While some of the designs have 2 × 2 MIMO capability in the low and middle-high bands,

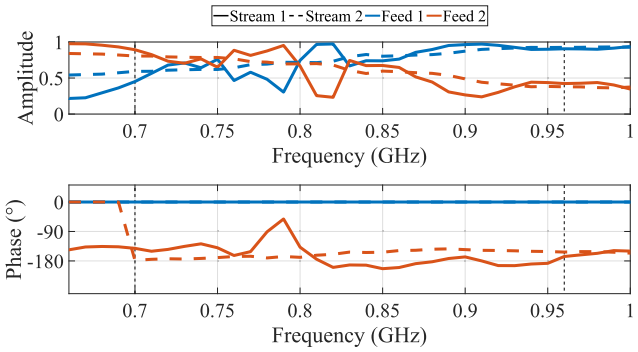

FIGURE 18. Feeding weights for the measured low band. Different data streams are indicated with different line types and the two feeds in a stream with different colors.

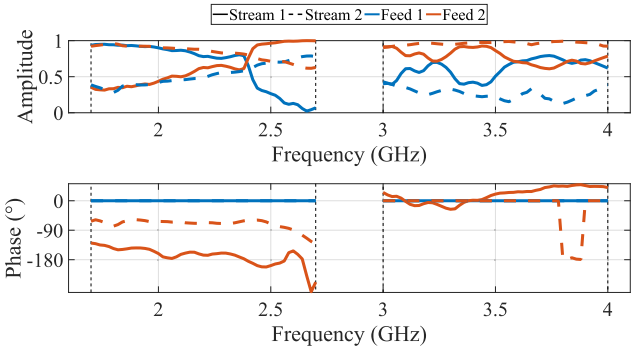

FIGURE 19. Feeding weights for streams 1 and 2 for the measured middle-high and high bands. Different data streams are indicated with different line types and the two feeds in a stream with different colors.

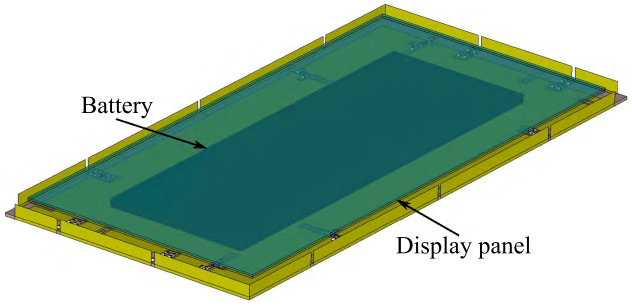

FIGURE 20. Simulation model with battery and display panel.

and some have 4×4 capability in either the middle-high or the high band, the proposed design is the only one capable in 2×2 MIMO operation in the low band and 4×4 MIMO operation both in the middle-high and the high bands. In addition, not all of the other designs can cover the 700 MHz band. Also, the proposed design has the smallest height of the antenna structure. When taking these factors into account, the comparison shows competitive performance.

B. SOME ADDITIONAL CONSIDERATIONS

Because of the switches needed to create the low band and high band structures, inter-band carrier aggregation (CA) cannot be directly used. However, it is possible to use one low band antenna simultaneously with two middle-high and high band antennas by using one half structure in the low band configuration and the other one in the middle-high and high band configuration. To simultaneously use all the antennas, the switches could be replaced with passive filter structures.

TABLE 3. Comparison of the proposed design with recent antenna designs.

Antenna	Clearance (mm)	Height (mm)	Frequency bands (GHz)	MIMO order	Efficiency (%)
Proposed	**5/3**	**4**	**LB: 0.7–0.96**	**2**	**30–40**
			MHB: 1.7–2.7	**4**	**50–70**
			HB: 3.0–4.0	**4**	**25–75**
[43]	13.5/0	5	LB: 0.824–0.96	2	37–54
			MHB: 1.7–2.7	4	55–73
[44]	2/2	7	LB: 0.82–0.96	1	40–52
			MHB: 1.7–2.7	1	45–90
			HB: 3.4–3.6	4	60–75
[4]	10/2	5	LB: 0.824–0.96	2	30–40
			MHB: 1.7–2.7	2	45–70
[5]	11/0	7	LB: 0.7–0.96	2	45–90
			MHB: 1.7–2.7	2	50–95
[33]	7/0	5	LB: 0.824–0.96	2	40–75
			MHB: 1.7–2.7	2	50–70
[45]	0/2	5	LB: 0.7–0.96	2	40–64
			MHB: 1.7–2.7	2	53–86
[46]	8/2	6	LB: 0.824–0.96	2	40–48
			MHB: 1.7–2.7	2	59–72
[24]	2/0	7	LB: 0.824–0.96	1	40–47
			MHB: 1.7–2.7	1	55–78
[27]	7/0	6	LB: 0.7–0.96	1	53–79
			MHB: 1.7–2.7	1	46–81

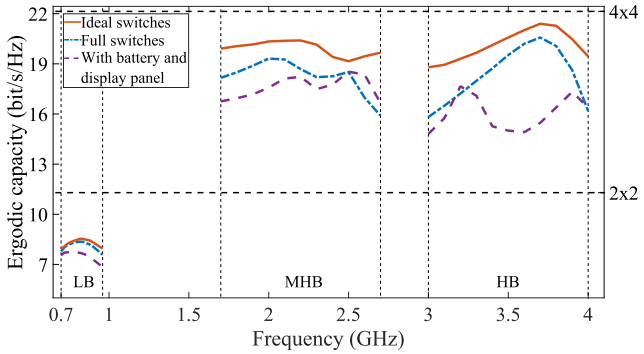

FIGURE 21. MIMO capacities calculated using simulated antenna properties for ideal switches, full switches, and for structure with battery and display panel.

To study how much the properties of the diodes and the bias networks affect the antenna performance, a comparison of the MIMO capacity for the realized switching circuits and ideal switches is performed with simulations. The ideal switches correspond to the structure of the switching circuits in Fig. 10 with the components replaced with either open or short circuits. In addition, the practical aspects of handset antennas are studied with a model that includes a battery and a display panel with the full switches. The battery is modelled with a 112×40×2.2 mm^3 PEC structure on top of the ground plane. The display panel is modelled with PEC and glass sheets with 140×69×1 mm^3 total size placed on top of the battery. The simulation model with the battery and display panel is shown in Fig. 20.

The resulting MIMO capacities for these three cases are shown in Fig. 21. Due to the low insertion loss of the diodes,

0.15 dB in the low band, the difference between the real and ideal switches is relatively small in the low band. The middle-high and high bands are affected more because the isolation of the diodes is 12–18 dB in these band. The results with the battery and the display panel show that the performance is slightly decreased in the low and middle-high bands and that the high-band performance is affected the most. Because the optimization of the structure was performed without these components, this decrease in the performance could be reduced by taking these components into account in the optimization process.

VII. CONCLUSION

A new antenna design method based on a multiport antenna simulation model combined with switches and an optimization algorithm has been presented in this paper. The developed method can evaluate a large number of different antenna structures in a short time thus making the design process faster. Because very few assumptions about the antenna structure are required, completely new and innovative antenna structures can easily be found.

The developed method has been applied to a mobile handset MIMO antenna design to prove its applicability. Manufactured and measured prototype shows competent performance. The results show that the antenna cluster concept can be used with low band antennas in mobile phone sized devices even with small ground clearances and large number of switches. The resulting antenna structure shows the potential of the proposed method in finding completely new antenna structures. Distributing the elements around the metal rim of the device is a solution that would have been difficult to find with traditional design methods.

The developed optimization method is promising already now, but it could also be further developed. By including the possibility to use matching circuits and reactive loading of the antenna elements, the performance could still be improved further. Also, the design process could be applied to more detailed phone models in the future.

REFERENCES

[1] A. C. K. Mak, C. R. Rowell, R. D. Murch, and C.-L. Mak, "Reconfigurable multiband antenna designs for wireless communication devices," *IEEE Trans. Antennas Propag.*, vol. 55, no. 7, pp. 1919–1928, Jul. 2007.

[2] C.-L. Lin and K.-L. Wong, "Printed monopole slot antenna for internal multiband mobile phone antenna," *IEEE Trans. Antennas Propag.*, vol. 55, no. 12, pp. 3690–3697, Dec. 2007.

[3] C.-H. Chang and K.-L. Wong, "Printed/8-PIFA for penta-band WWAN operation in mobile phone," *IEEE Trans. Antennas Propag.*, vol. 57, no. 5, pp. 1373–1381, May 2009.

[4] L. W. Zhang, Y. L. Ban, C. Y. D. Sim, J. Guo, and Z. F. Yu, "Parallel dual-loop antenna for WWAN/LTE metal-rimmed smartphone," *IEEE Trans. Antennas Propag.*, vol. 66, no. 3, pp. 1217–1226, Mar. 2018.

[5] M. Stanley, Y. Huang, H. Wang, H. Zhou, Z. Tian, and Q. Xu, "A novel reconfigurable metal rim integrated open slot antenna for Octa-Band smartphone applications," *IEEE Trans. Antennas Propag.*, vol. 65, no. 7, pp. 3352–3363, Jul. 2017.

[6] A. Cabedo, J. Anguera, C. Picher, M. Ribo, and C. Puente, "Multiband handset antenna combining a PIFA, slots, and ground plane modes," *IEEE Trans. Antennas Propag.*, vol. 57, no. 9, pp. 2526–2533, Sep. 2009.

[7] F.-H. Chu and K.-L. Wong, "Internal coupled-fed dual-loop antenna integrated with a USB connector for WWAN/LTE mobile handset," *IEEE Trans. Antennas Propag.*, vol. 59, no. 11, pp. 4215–4221, Nov. 2011.

[8] Y. Li, Z. Zhang, J. Zheng, Z. Feng, and M. F. Iskander, "A compact hepta-band loop-inverted f reconfigurable antenna for mobile phone," *IEEE Trans. Antennas Propag.*, vol. 60, no. 1, pp. 389–392, Jan. 2012.

[9] M. Zheng, H. Wang, and Y. Hao, "Internal hexa-band folded monopole/dipole/loop antenna with four resonances for mobile device," *IEEE Trans. Antennas Propag.*, vol. 60, no. 6, pp. 2880–2885, Jun. 2012.

[10] Y.-L. Ban, J.-H. Chen, S. Yang, J. L.-W. Li, and Y.-J. Wu, "Low-profile printed octa-band LTE/WWAN mobile phone antenna using embedded parallel resonant structure," *IEEE Trans. Antennas Propag.*, vol. 61, no. 7, pp. 3889–3894, Jul. 2013.

[11] S. A. Ja'afreh, Y. Huang, and L. Xing, "Low profile and wideband planar inverted-F antenna with polarisation and pattern diversities," *IET Microw., Antennas Propag.*, vol. 10, no. 2, pp. 152–161, Jan. 2016.

[12] K.-L. Wong, C.-C. Wan, and L.-Y. Chen, "Self-decoupled compact metal-frame LTE MIMO antennas for the smartphone," *Microw. Opt. Technol. Lett.*, vol. 60, no. 5, pp. 1170–1179, May 2018.

[13] P. Vainikainen, J. Ollikainen, O. Kivekas, and K. Kelander, "Resonator-based analysis of the combination of mobile handset antenna and chassis," *IEEE Trans. Antennas Propag.*, vol. 50, no. 10, pp. 1433–1444, Oct. 2002.

[14] A. Lehtovuori, R. Valkonen, and J. Ilvonen, "Designing capacitive coupling element antennas with bandwidth estimators," *IEEE Antennas Wireless Propag. Lett.*, vol. 13, pp. 959–962, 2014.

[15] J. Ilvonen, R. Valkonen, J. Holopainen, and V. Viikari, "Design strategy for 4G handset antennas and a multiband hybrid antenna," *IEEE Trans. Antennas Propag.*, vol. 62, no. 4, pp. 1918–1927, Apr. 2014.

[16] M. Cismasu and M. Gustafsson, "Antenna bandwidth optimization with single frequency simulation," *IEEE Trans. Antennas Propag.*, vol. 62, no. 3, pp. 1304–1311, Mar. 2014.

[17] E. Hassan, E. Wadbro, and M. Berggren, "Topology optimization of metallic antennas," *IEEE Trans. Antennas Propag.*, vol. 62, no. 5, pp. 2488–2500, May 2014.

[18] R. Luomaniemi, "Switch-based frequency-reconfigurable MIMO antennas for handsets," M.S. thesis, Aalto Univ., Espoo, Finland, 2018.

[19] Q. Guo, R. Mittra, F. Lei, Z. Li, J. Ju, and J. Byun, "Interaction between internal antenna and external antenna of mobile phone and hand effect," *IEEE Trans. Antennas Propag.*, vol. 61, no. 2, pp. 862–870, Feb. 2013.

[20] B. Yuan, Y. Cao, G. Wang, and B. Cui, "Slot antenna for metal-rimmed mobile handsets," *IEEE Antennas Wireless Propag. Lett.*, vol. 11, pp. 1334–1337, 2012.

[21] J. Zhong, K.-K. Chen, and X. Sun, "A novel multi-band antenna for mobile phone with metal frame," in *Proc. IEEE 8th Int. Conf. Wireless Commun., Netw. Mobile Comput.*, Sep. 2012, pp. 1–4.

[22] Y. L. Ban, Y. F. Qiang, Z. Chen, K. Kang, and J. H. Guo, "A Dual-Loop antenna design for hepta-band WWAN/LTE metal-rimmed smartphone applications," *IEEE Trans. Antennas Propag.*, vol. 63, no. 1, pp. 48–58, Jan. 2015.

[23] C.-K Hsu and S.-J. Chung, "Compact multiband antenna for handsets with a conducting edge," *IEEE Trans. Antennas Propag.*, vol. 63, no. 11, pp. 5102–5107, Nov. 2015.

[24] K.-L. Wong and Y.-C. Wu, "Small-size dual-wideband IFA frame antenna closely integrated with metal casing of the LTE smartphone and having decreased user's hand effects," *Microw. Opt. Technol. Lett.*, vol. 58, no. 12, pp. 2853–2858, Dec. 2016.

[25] J. Lian, Y. Ban, Y. Yang, L. Zhang, C. Sim, and K. Kang, "Hybrid multi-mode narrow-frame antenna for WWAN/LTE metal-rimmed smartphone applications," *IEEE Access*, vol. 4, pp. 3991–3998, 2016.

[26] H. Chen and A. Zhao, "LTE antenna design for mobile phone with metal frame," *IEEE Antennas Wireless Propag. Lett.*, vol. 15, pp. 1462–1465, 2016.

[27] D. Huang and Z. Du, "Eight-band antenna with a small ground clearance for LTE metal-frame mobile phone applications," *IEEE Antennas Wireless Propag. Lett.*, vol. 17, no. 1, pp. 34–37, Jan. 2018.

[28] J. Kurvinen, A. Lehtovuori, J. Mai, C. Wang, and V. Viikari, "Metal-covered handset with LTE MIMO, WI-FI MIMO, and GPS antennas," *Prog. Electromagn. Res. C*, vol. 80, no. 13, pp. 89–101, 2018.

[29] J.-M. Hannula, J. Holopainen, and V. Viikari, "Concept for frequency-reconfigurable antenna based on distributed transceivers," *IEEE Antennas Wireless Propag. Lett.*, vol. 16, pp. 764–767, 2016.

[30] J.-M. Hannula, T. Saarinen, J. Holopainen, and V. Viikari, "Frequency reconfigurable multiband handset antenna based on a multichannel transceiver," *IEEE Trans. Antennas Propag.*, vol. 65, no. 9, pp. 4452–4460, Sep. 2017.
[31] J.-M. Hannula *et al.*, "Performance analysis of frequency-reconfigurable antenna cluster with integrated radio transceivers," *IEEE Antennas Wireless Propag. Lett.*, vol. 17, no. 5, pp. 756–759, May 2018.
[32] J.-M. Hannula, T. O. Saarinen, A. Lehtovuori, J. Holopainen, and V. Viikari, "Tunable eight-element MIMO antenna based on the antenna cluster concept," *IET Microw., Antennas Propag.*, to be published.
[33] Y.-L. Ban, Y.-F. Qiang, G. Wu, H. Wang, and K.-L. Wong, "Reconfigurable narrow-frame antenna for LTE/WWAN metal-rimmed smartphone applications," *IET Microw., Antennas Propag.*, vol. 10, no. 10, pp. 1092–1100, Jul. 2016.
[34] C. Volmer, M. Sengul, J. Weber, R. Stephan, and M. A. Hein, "Broadband decoupling and matching of a superdirective two-port antenna array," *IEEE Antennas Wireless Propag. Lett.*, vol. 7, pp. 613–616, 2008.
[35] R. Tian, B. K. Lau, and Z. Ying, "Multiplexing efficiency of MIMO antennas," *IEEE Antennas Wireless Propag. Lett.*, vol. 10, pp. 183–186, 2011.
[36] H. Shin and J. H. Lee, "Closed-form formulas for ergodic capacity of MIMO Rayleigh fading channels," in *Proc. IEEE Int. Conf. Commun.*, May 2003, pp. 2996–3000.
[37] Y.-L. Ban, C. Li, C.-Y.-D. Sim, G. Wu, and K.-L Wong, "4G/5G multiple antennas for future multi-mode smartphone applications," *IEEE Access*, vol. 4, pp. 2981–2988, 2016.
[38] K.-L. Wong, C.-Y. Tsai, and J.-Y. Lu, "Two asymmetrically mirrored gap-coupled loop antennas as a compact building block for eight-antenna MIMO array in the future smartphone," *IEEE Trans. Antennas Propag.*, vol. 65, no. 4, pp. 1765–1778, Apr. 2017.
[39] A. Lehtovuori, J. Ilvonen, K. Rasilainen, and V. Viikari, "Single-element handset antenna design for modern smartphones: An industrial approach," in *Proc. 11th Eur. Conf. Antennas Propag. (EUCAP)*, Mar. 2017, pp. 2960–2963.
[40] *Understanding RF/Microwave Solid State Switches and Their Applications*, Keysight Technol., Santa Rosa, CA, USA, 2016.
[41] G. M. Rebeiz and J. B. Muldavin, "RF MEMS switches and switch circuits," *IEEE Microw. Mag.*, vol. 2, no. 4, pp. 59–71, Dec. 2001.
[42] D. M. Pozar, *Microwave Engineering*, 4th ed. Hoboken, NJ, USA: Wiley, 2012.
[43] Y.-H. Zhang, S.-R. Yang, Y.-L. Ban, Y.-F. Qiang, J. Guo, and Z.-F. Yu, "Four-feed reconfigurable MIMO antenna for metal-frame smartphone applications," *IET Microw., Antennas Propag.*, vol. 12, no. 9, pp. 1477–1482, Jul. 2018.
[44] Q. Chen *et al.*, "Single ring slot-based antennas for metal-rimmed 4G/5G smartphones," *IEEE Trans. Antennas Propag.*, vol. 67, no. 3, pp. 1476–1487, Mar. 2019.
[45] J. Choi, W. Hwang, C. You, B. Jung, and W. Hong, "Four-element reconfigurable coupled loop MIMO antenna featuring LTE full-band operation for metallic-rimmed smartphone," *IEEE Trans. Antennas Propag.*, vol. 67, no. 1, pp. 99–107, Jan. 2019.
[46] Z.-Q. Xu, Y. Sun, Q.-Q. Zhou, Y.-L. Ban, Y.-X. Li, and S. S. Ang, "Reconfigurable MIMO antenna for integrated-metal-rimmed smartphone applications," *IEEE Access*, vol. 5, pp. 21223–21228, 2017.

RASMUS LUOMANIEMI (S'16) was born in Salo, Finland, in 1994. He received the B.Sc. (Tech.) (Hons.) and M.Sc. (Tech.) (Hons.) degrees in electrical engineering from Aalto University, Espoo, Finland, in 2016 and 2018, respectively, where he is currently pursuing the D.Sc. (Tech.) degree.

He has been with the Department of Electronics and Nanoengineering, Aalto University School of Electrical Engineering, since 2014, where he is currently pursuing the D.Sc. degree. His current research interest includes MIMO antennas for mobile devices.

Mr. Luomaniemi was a recipient of the Second Prize in the IEEE AP-S Student Design Contest as a part of the Team Aalto ELEC, in 2016.

JARI-MATTI HANNULA (S'16–M'18) was born in Luvia, Finland, in 1990. He received the B.Sc. (Tech.) (Hons.), M.Sc. (Tech.) (Hons.), and D.Sc. (Tech.) (Hons.) degrees in electrical engineering from Aalto University School of Electrical Engineering, Espoo, Finland, in 2014, 2015, and 2018, respectively.

Since 2013, he has been with the Department of Electronics and Nanoengineering, Aalto University School of Electrical Engineering, Espoo, where he is currently a Postdoctoral Researcher. His current research interests include analysis of multiantenna systems and antenna-transceiver codesign.

ANU LEHTOVUORI received the M.Sc. (Tech.) and Lic.Sc. (Tech.) degrees from the Helsinki University of Technology, Espoo, Finland, in 2000 and 2003, respectively, and the D.Sc. (Tech.) degree from Aalto University, Espoo, in 2015, all in electrical engineering.

She is currently a University Lecturer in circuit theory with the Aalto University School of Electrical Engineering, Espoo. Her current research interests include electrically small antennas and design of antennas for mobile devices.

VILLE VIIKARI (S'06–A'09–M'09–SM'10) was born in Espoo, Finland, in 1979. He received the M.Sc. (Tech.) and D.Sc. (Tech.) (Hons.) degrees in electrical engineering from the Helsinki University of Technology (TKK), Espoo, Finland, in 2004 and 2007, respectively.

He is currently an Associate Professor and the Deputy Head of the Department with the Aalto University School of Electrical Engineering, Espoo. From 2001 to 2007, he was with the Radio Laboratory, TKK, where he studied antenna measurement techniques at submillimeter wavelengths and antenna pattern correction techniques. From 2007 to 2012, he was a Research Scientist and a Senior Scientist with the VTT Technical Research Centre, Espoo, Finland, where his research included wireless sensors, RFID, radar applications, MEMS, and microwave sensors. His current research interests include antennas for mobile networks, RF-powered devices, and antenna measurement techniques.

Dr. Viikari was a recipient of the Young Researcher Award of the Year 2014, presented by the Finnish Foundation for Technology Promotion, the IEEE Sensors Council 2010 Early Career Gold Award, the 2008 Young Scientist Award of the URSI XXXI Finnish Convention on Radio Science, Espoo, Finland, and the Best Student Paper Award of the annual symposium of the Antenna Measurement Techniques Association, Newport, RI, USA, in 2005. He has served as the Chair of the Technical Program Committee of the ESA Workshop on Millimetre-Wave Technology and Applications and the Global Symposium on Millimeter Waves (GSMM) twice, in Espoo, Finland, in 2011 and 2016, respectively.